Available online at www.sciencedirect.com
ScienceDirect
Signal Processing 87 (2007) 148–161
SIGNAL PROCESSING
www.elsevier.com/locate/sigpro

New blind frequency offset estimator for OFDM systems over frequency selective fading channels

Ronghong Mo[a], Yong Huat Chew[b,*], Tjeng Thiang Tjhung[b], Chi Chung Ko[a]

[a]*Department of Electrical Engineering, National University of Singapore, 10 Kent Ridge Crescent, Singapore 119260, Singapore*
[b]*Institute for Infocomm Research, Agency of Science, Technology and Research, 21 Heng Mui Keng Terrace, Singapore 119613, Singapore*

Received 2 April 2005; received in revised form 28 April 2006; accepted 4 May 2006
Available online 12 June 2006

Abstract

In this paper, a blind frequency offset estimator for orthogonal frequency division multiplexing (OFDM) systems over frequency selective fading channels based on modeling the unknown channel fading gains as deterministic variables is proposed. In this estimator, the received time domain OFDM samples are first partitioned into subsets, in which neighboring samples are uncorrelated, leading to a tri-diagonal signal correlation matrix for each subset. The ML cost functions from each of the subsets are combined to perform frequency offset estimation. Simulation results show that the proposed frequency offset estimator achieves better performance than the estimators reported in [J.-J. Van De Beek, M. Sandell, P.O. Borjesson, ML estimation of time and frequency offset in OFDM systems, IEEE Trans. Signal Process. 45 (July 1997) 1800–1805] and [X. Ma, G.B. Giannakis, S. Barbarossa, Non-data-aided frequency-offset and channel estimation in OFDM: and related block transmission, IEEE ICC'01, June 2001, pp. 1866–1870]. Moreover, although the power delay profile needs to be known in deriving the proposed estimator, simulation and analytical results show that the performance of the proposed estimator is not sensitive to variation in the power delay profile.

Keywords: Blind frequency offset estimator; Maximum likelihood; OFDM; Frequency selective fading channel; Frequency synchronization

1. Introduction

Orthogonal frequency division multiplexing (OFDM) systems are vulnerable to frequency synchronization errors that result in the loss of orthogonality among subcarriers and thus the substantial degradation of error probability performance. Therefore, frequency offset needs to be estimated and compensated before symbol detection is performed.

Blind frequency offset estimators, which do not rely on the transmission of pilot symbols, have recently received considerable attention because they are bandwidth efficient. In [1], a maximum likelihood (ML)-based blind joint symbol timing and frequency offset estimator was studied for OFDM systems over additive white Gaussian noise (AWGN) channel, based on modeling the transmitted OFDM signals as Gaussian

*Corresponding author. Tel.: +65 68745681.
E-mail address: chewyh@i2r.a-star.edu.sg (Y.H. Chew).

0165-1684/$ - see front matter © 2006 Elsevier B.V. All rights reserved.
doi:10.1016/j.sigpro.2006.05.003

random variables. In [2], a blind joint estimator similar to that in [1] was proposed based on assuming that the received OFDM signals over time varying frequency selective fading channels can also be modeled as Gaussian random variables. In [3], a correlation-based frequency offset estimator was proposed by exploiting the redundancy of cyclic prefix (CP). In [4], a blind frequency offset estimator utilizing the phase shift introduced by the presence of frequency offset was obtained for OFDM systems with unused subcarriers (virtual subcarriers), and by oversampling the received OFDM signals by a factor of two. All these above mentioned estimators were either frequency offset or joint symbol timing and frequency offset estimators, which are derived based on only one or two received OFDM symbols. In contrast, for several other blind estimators reported in the literature, observation of multiple OFDM symbols at the receiver is needed to guarantee the estimation performance. In [5,6], a subspace-based blind estimator and its equivalent ML-based frequency estimator that take advantage of virtual subcarriers were investigated. In [7], an estimator based on the second order cyclostationarity of received signals was proposed, where a few 100 OFDM symbols were observed to guarantee the estimation performance. A feedback frequency offset estimator, where the ML estimate is obtained iteratively, was proposed in [8]. In general, to obtain the frequency offset estimate, some estimators need the knowledge of SNR and power delay profile to perform estimation [1,8,2], while for some other estimators, such information is not required [3–7].

Fast ML-based blind frequency offset estimators that observe only one OFDM symbol to achieve reliable estimation are desirable for applications with stringent delay requirement. The blind estimator studied in [1] was derived for AWGN channels. It works reliably in AWGN channels, but its performance is degraded considerably when used over frequency selective fading channels. In order to obtain a ML cost function leading to an estimator with closed form expression for frequency selective fading channels, Lv et al. [2] removed the need to specify the distribution of the channel gains by approximating the received OFDM signals as Gaussian random variables. In this paper, we propose a blind frequency offset estimator that is also based on one received OFDM symbol. In this proposed estimator, channel gains are treated as deterministic unknown variables estimated together with the frequency offset. However, conditioned on channel fading gains, the signal correlation matrix with many non-zero entries is expected since neighboring received OFDM samples are correlated in the presence of multipath, and an ML estimator with closed form expression is difficult to obtain. In order to solve this problem, we propose to partition the received time domain OFDM samples into a few subsets, in which neighboring samples are uncorrelated. The partitioning and reconstruction of the received OFDM samples result in a tri-diagonal signal correlation matrix for each subset leading to a practical estimation algorithm. The details on the partitioning of the received samples into subsets and the derivation of the proposed estimator based on these subsets will be elaborated in Section 2. Its performance will be compared with that of the estimators reported in [1,3] in Section 3.

2. Proposed estimators

Consider an OFDM transmission over frequency selective fading channels. The maximum delay spread (normalized to $T_s = 1/B$, where B is the OFDM system bandwidth) is L. The CP with length of N_g samples is appended to the beginning of each OFDM symbol. Normally, $N_g \geqslant L$ is assumed to avoid inter-symbol interference and the resultant redundancy can be used to perform efficient synchronization [9]. We assume that the symbol timing synchronization of the OFDM system has been achieved so that the receiver knows exactly where the OFDM symbol starts. A complete OFDM symbol containing $N + N_g$ samples is observed. The received samples for one OFDM symbol can be written in a compact vector form as

$$\mathbf{r} = [r_1, r_2, \ldots, r_{N_g}, \ldots, r_{N+N_g}], \tag{1}$$

where the kth received sample is given by

$$r_k = \sum_{l=0}^{L_p-1} h_l s_{k-l} e^{j(2\pi k\varepsilon/N)} + w_k, \quad k = 1, \ldots, N + N_g. \tag{2}$$

The symbol s_k in (2) denotes the transmitted time domain signal sample and $\sigma_s^2 = E[s_k s_k^*]$ is the symbol energy. The transmitted signal s_k can be modeled as a Gaussian random variable but not white due to the existence of

CP [1]. The channel fading gain for the lth path, h_l (for $l = 0, \ldots, L_p - 1$), is assumed to be a complex Gaussian random variable with variance σ_l^2. We consider a slow fading channel so that h_l remains unchanged over a few OFDM symbols. h_l for different paths is independent of each other. The parameter L_p denotes the instantaneous number of delay paths and might vary with changing transmission environments. Normally, for most mobile applications, the knowledge of L_p is not known a priori, unless it is estimated instantaneously at the receiver. w_k is AWGN with variance σ_w^2, and ε is the normalized frequency offset and $|\varepsilon| \leqslant \frac{1}{2}$.

From (2), it can be seen that the received OFDM signal is not exactly Gaussian distributed, because it is the sum of products between two Gaussian distributed random variables h_l and s_k. However, conditioned on channel fading gains h_l, r_k is a Gaussian random variable. If h_ls are treated as nuisance parameters (which do not need to be estimated), the conventional ML (or unconditional ML, UML) cost function is given as [10]

$$\Lambda(\mathbf{r}|\varepsilon) = \int_{\mathbf{h}} \Lambda(\mathbf{r}|\varepsilon, \mathbf{h}) f_{\mathbf{h}}(\mathbf{h})\, \mathrm{d}\mathbf{h}, \tag{3}$$

where

$$\Lambda(\mathbf{r}|\varepsilon, \mathbf{h}) = \frac{1}{\pi^{N+N_g}|\mathbf{C}_{\mathbf{h}}|}\, \mathrm{e}^{-\mathbf{r}^{\mathrm{H}}\mathbf{C}_{\mathbf{h}}^{-1}\mathbf{r}} \tag{4}$$

is the conditional ML (CML) cost function conditioned on $\mathbf{h}$. It can be seen that the CML cost function is obtained by treating $\mathbf{h}$ as deterministic instead of random variables. $f_{\mathbf{h}}(\mathbf{h})$ is the joint probability density function (p.d.f.) of $\mathbf{h}$. The superscript $(\cdot)^{\mathrm{H}}$ denotes complex conjugate transpose. $\mathbf{C}_{\mathbf{h}} = E_{\mathbf{h}}[\mathbf{r}\mathbf{r}^{\mathrm{H}}]$ is the $(N + N_g) \times (N + N_g)$ signal correlation matrix conditioned on the fading gains $\mathbf{h} = [h_0, \ldots, h_{L_p-1}]$.

The (i,k)th element, $\mathbf{C}_{\mathbf{h}}(i,k)$, of signal correlation matrix $\mathbf{C}_{\mathbf{h}}$, is given as

$$\mathbf{C}_{\mathbf{h}}(j,k) = \begin{cases} \sigma_s^2 \sum_{l=0}^{L_p-(k-i)-1} h_l h_{l+(k-i)}^* & \\ \quad \mathrm{e}^{-\mathrm{j}2\pi(k-i)\varepsilon/N} + \sigma_w^2 \delta(i-k) & \forall\, 0 \leqslant k-i \leqslant L_p - 1, \\ \sigma_s^2 \sum_{l=0}^{i-1} |h_l|^2 \mathrm{e}^{-\mathrm{j}2\pi\varepsilon} & \forall\, 1 \leqslant i \leqslant L_p - 1,\ \ k = i + N, \\ \sigma_s^2 \sum_{l=0}^{L_p-1} |h_l|^2 \mathrm{e}^{-\mathrm{j}2\pi\varepsilon} & \forall\, L_p \leqslant i \leqslant N_g,\ \ k = i + N, \\ \sigma_s^2 \sum_{l=i-L_p}^{L_p-1} |h_l|^2 \mathrm{e}^{-\mathrm{j}2\pi\varepsilon} & \forall\, N_g + 1 \leqslant i \leqslant N_g + L_p - 1,\ \ k = i + N, \\ 0 & \text{otherwise.} \end{cases} \tag{5}$$

In (5), we only show the upper diagonal elements with $k > i$. However we should note that $\mathbf{C}_{\mathbf{h}}(k,i) = \mathbf{C}_{\mathbf{h}}^*(i,k)$, where $(\cdot)^*$ denotes the complex conjugate.

The frequency offset estimator based on (3) is obtained as

$$\hat{\varepsilon} = \arg \max_{\varepsilon} \Lambda(\mathbf{r}|\varepsilon). \tag{6}$$

Due to the complicated form of the matrix $\mathbf{C}_{\mathbf{h}}$ and the multi-variable integration in (3), it is difficult to simplify (6) into a form easy for implementation. An approach to remove the need to specify the p.d.f. of $\mathbf{h}$ in the UML cost function in (3) is to directly assume that the received signal is approximately Gaussian distributed, as in [2]. This will then result in a simpler ML cost function similar to that in [1] for AWGN channel.

Now we examine the estimators based on the CML approach, where h_ls (for $l = 0, \ldots, L_p - 1$) are treated as deterministic variables estimated together with the frequency offset. The ML cost functions of the new estimator are thus given by (4), rather than by (3) where h_ls are modeled as random variables. The joint channel and frequency offset estimator is thus given as

$$\hat{\varepsilon}, \hat{\mathbf{h}} = \arg \max_{\varepsilon, \mathbf{h}} \Lambda(\mathbf{r}|\varepsilon, \mathbf{h}). \tag{7}$$

However, from (4) and (5), we can also see that a closed form expression for this joint estimator is difficult to obtain since the neighboring OFDM samples are correlated as shown in (2).

Therefore, we propose a method to obtain a practical frequency offset estimator based on the CML approach. In this new estimator, we partition the received signal samples of the observed OFDM symbol given in (1) into a number of subsets. The frequency offset estimate is derived based on the CML cost function of the

resulting subsets. We will show that the new frequency estimator can be expressed in a closed form and thus can be implemented easily.

2.1. Partitioning of OFDM signals

Ideally, the subset is constructed by picking up the OFDM received samples given in (1) separated by a number of L_p samples. However, in this paper, we assume that L_p which describes the instantaneous number of delay paths is not estimated and hence its value is not available at the receiver. To cater for the variation of L_p with changing transmission environments, each subset is formed by picking up the received OFDM samples separated by the maximum number of delay paths L (rather than L_p), as shown in Fig. 1. To this end, the knowledge of L is a prerequisite. The effect of $L_p < L$ on the accuracy of the estimator will be investigated in Section 3.

With this partitioning, the vector given in (1) is now divided into a number of $(2L-1)$ non-overlapping subsets. In the following, we show that, for the mth subset, the signal correlation matrix $\mathbf{C}_{\mathbf{h},m}$ becomes tri-diagonal, for $m = 1, \ldots, L$. Hence, an estimator with closed form expression can be easily obtained based on $\mathbf{C}_{\mathbf{h},m}$, $m = 1, \ldots, 2L-1$.

Assuming that $v = N_g - PL$, where $P = \lfloor N_g/L \rfloor$, and $\lfloor x \rfloor$ denotes the largest integer smaller than x. For $m = 1, \ldots, (2L-1)$, the subsets $\mathbf{r}_m$ obtained after the partitioning are shown as follows:

(1) For $m = 1$

$$\mathbf{r}_1 = [\underbrace{r_L, r_{2L}, \ldots, r_{PL}}_{P \text{ ISI free CP samples}, I_1}, \ldots, r_{QL}, \underbrace{r_{L+N}, r_{2L+N}, \ldots, r_{PL+N}}_{P \text{ data samples}, I'_1}]. \tag{8}$$

Here $Q = \lfloor N/L \rfloor$ denotes the number of samples between the first ISI free sample and its data replica in each subset.

(2) For $m = 2, \ldots, v+1$

$$\mathbf{r}_m = [\underbrace{r_{L+m-1}, r_{2L+m-1}, \ldots, r_{PL+m-1}}_{P \text{ ISI free CP samples}, I_m}, \ldots, r_{(Q-1)L+m-1}, \underbrace{r_{L+N+m-1}, r_{2L+N+m-1}, \ldots, r_{PL+N+m-1}}_{P \text{ data samples}, I'_m}]. \tag{9}$$

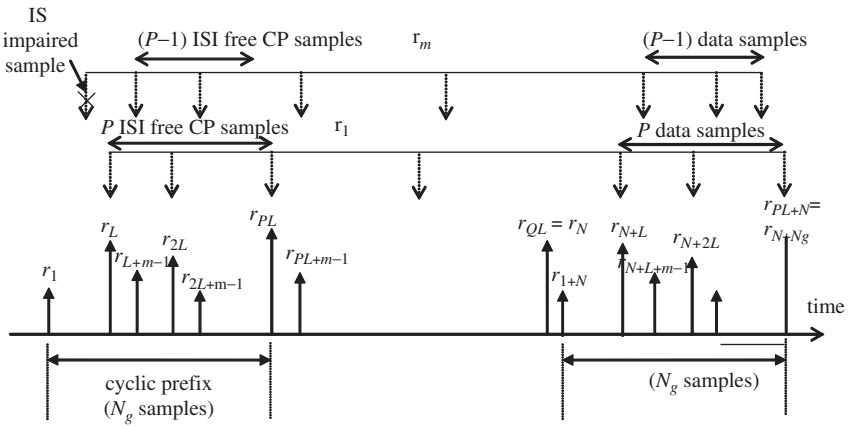

Fig. 1. Illustration of sub-vector $\mathbf{r}_m$ for $Q = N/L, v = 0$.

(3) For $m = v+2, \ldots, L$

$$\mathbf{r}_m = [\underbrace{r_{L+m-1}, r_{2L+m-1}, \ldots, r_{(P-1)L+m-1}}_{(P-1)\text{ ISI free CP samples}, I_m}, \ldots, r_{(Q-1)L+m-1},$$
$$\underbrace{r_{L+N+m-1}, r_{2L+N+m-1}, \ldots, r_{(P-1)L+N+m-1}}_{(P-1)\text{ data samples}, I'_m}]. \tag{10}$$

(4) For $m = L+1, \ldots, 2L-1$

$$\mathbf{r}_m = [r_{m-L}, r_{m-L+N}]. \tag{11}$$

In (8)–(10), the sets "I_m" and "I'_m" denote the ISI free CP samples and their data replicas contained in the mth subset, respectively. For example, $I_m = \{r_{L+m-1}, \ldots, r_{(P-1)L+m-1}\}$ and $I'_m = \{r_{L+N+m-1}, \ldots, r_{(P-1)L+N+m-1}\}$ in (10). In these subsets, in order to maintain a neat cross correlation matrix as shown later in this section, the received OFDM samples from r_1 to r_{L-1} and from r_{N+1} to r_{N+L-1} are not included. Furthermore, the samples r_{QL} and r_{L+N} in (8), and the samples $r_{(Q-1)L+m-1}$ and $r_{L+N+m-1}$ in (9) and (10), might be separated by more than L samples if $Q = \lfloor N/L \rfloor \neq N/L$. This is because we need to maintain the correlation between r_L and r_{L+N} in (8), and the correlation between r_{L+m-1} and $r_{L+N+m-1}$ in (9) and (10). It should also be noted that, in (8) and (9), the samples r_{N+m-1} are removed, since these samples are included in the subsets given in (11). For example, for $m = 2$ and $N = QL$, $r_{QL+m-1} = r_{N+1}$, which is also the sample contained in (11) for $m = L+1$.

From (8) to (11), we see that the received samples for one OFDM symbol are now divided into $2L-1$ subsets.

Among the first L subsets, there are $(v+1)$ subsets containing a number of P ISI free CP samples as shown in (8) and (9), and the remaining $(L-v-1)$ subsets have $(P-1)$ ISI free CP samples as shown in (10). The illustration of $\mathbf{r}_1, \mathbf{r}_m$ (where $v+2 \leqslant m \leqslant L$) for $N = QL$ and $v = 0$ are shown in Fig. 1.

The subsets given in (11) contain the received OFDM samples from r_1 to r_{L-1}, which are corrupted by the preceding OFDM symbol. However, since these samples contain the transmitted CP samples, in our algorithm they will also be exploited to estimate the frequency offset.

With the above partitioning, for $m = 1, \ldots, L$, the signal correlation matrix $\mathbf{C}_{\mathbf{h},m}$ for subset $\mathbf{r}_m$, conditioned on h_l $(l = 0, \ldots, L_p - 1)$ and ε is given as follows:

$$\mathbf{C}_{\mathbf{h},m}(i,k) = \begin{cases} \sigma_s^2 \sum_{l=0}^{L_p-1} |h_l|^2 + \sigma_w^2, & k = i, \\ \sigma_s^2 \sum_{l=0}^{L_p-1} |h_l|^2 \mathrm{e}^{-\mathrm{j}2\pi\varepsilon}, & k = i+Q, \\ 0 & \text{otherwise.} \end{cases} \tag{12}$$

Note that, unlike (5), (12) has non-zero elements in only three diagonals. Our approach now becomes clear that it is to partition the OFDM samples into subsets that consist of uncorrelated neighboring samples. Therefore, each subset has a signal correlation matrix which is similar to that reported in [1] for AWGN channels, however, is a function of h_l in our case. Without such partitioning, the estimator proposed in [1] cannot be extended to OFDM systems over frequency selective fading channels, since the received time domain OFDM samples are correlated as shown by (5) and thus it is impossible to obtain a ML cost function having the form of the ML function reported in [1].

For $m \in \{L+1, \ldots, 2L-1\}$, the signal correlation matrix $\mathbf{C}_{\mathbf{h},m}$ has a dimension of 2×2 and its elements are given by

$$\mathbf{C}_{\mathbf{h},m}(i,k) = \begin{cases} \sigma_s^2 \sum_{l=0}^{L_p-1} |h_l|^2 + \sigma_w^2, & k = i, \\ \sigma_s^2 \sum_{l=0}^{m-L_p-1} |h_l|^2 \mathrm{e}^{-\mathrm{j}2\pi\varepsilon}, & k = i+1. \end{cases} \tag{13}$$

2.2. Computation of cost function for $\mathbf{r}_m$

After the above partitioning, substituting (12) into (4) and with some manipulations, conditioned on ε and γ, where

$$\gamma = \frac{\sigma_s^2}{\sigma_w^2} \sum_{l=0}^{L_p-1} |h_l|^2, \tag{14}$$

the ML cost function for $\mathbf{r}_m$ (for $m = 1, \ldots, L$) can be expressed as

$$\begin{aligned} \Lambda^{(1)}(\mathbf{r}_m|\varepsilon,\gamma) = & \prod_{k\notin I_m\cup I'_m} \frac{1}{\pi\sigma_w^2(\gamma+1)} \mathrm{e}^{-|r_m(k)|^2/(\sigma_w^2(\gamma+1))} \\ & \times \prod_{k\in I_m} \frac{1}{\pi^2\sigma_w^4(2\gamma+1)} \times \mathrm{e}^{-[(\gamma+1)(|r_m(k)|^2+|r_m(k+Q)|^2)-2\gamma Re\{\mathrm{e}^{\mathrm{j}2\pi\varepsilon} r_m(k) r_m^*(k+Q)\}]/\sigma_w^2(2\gamma+1)}, \end{aligned} \tag{15}$$

where $r_m(k)$ denotes the kth element of $\mathbf{r}_m$.

In (15), since the ML function can be expressed as a function of γ, the conditional ML on $\mathbf{h}$ can now be changed to the conditional ML on γ. The ML cost function given in (15) now has a much simpler form than the one given in (7) which involves the signal correlation matrix given in (5). This is the direct consequence of the uncorrelatedness of the neighboring samples in each subset.

Likewise, substituting (13) into (4), the ML cost function for $\mathbf{r}_m$ where $m = L+1, \ldots, 2L+1$ is given as

$$\begin{aligned} \Lambda^{(2)}(\mathbf{r}_m|\varepsilon,\gamma,\gamma_{1,m}) = & \frac{1}{\pi^2\sigma_w^4(\gamma^2+2\gamma+1-\gamma_{1,m}^2)} \\ & \times \mathrm{e}^{-[(\gamma+1)(|r_{m-L}|^2+|r_{m-L+N}|^2)-2\gamma_{1,m} Re\{\mathrm{e}^{\mathrm{j}2\pi\varepsilon} r_{m-L} r_{m-L+N}^*\}]/\sigma_w^2(\gamma^2+2\gamma+1-\gamma_{1,m}^2)}, \end{aligned} \tag{16}$$

where

$$\gamma_{1,m} = \frac{\sigma_s^2}{\sigma_w^2} \sum_{l=0}^{m-L-1} |h_l|^2. \tag{17}$$

Since each subset consists of only two samples, r_{m-L} and r_{m-L+N}, (16) is much simpler than (15).

After omitting the constant terms, the log-likelihood function of (15) can be simplified as

$$\begin{aligned} \Lambda_{\log}^{(1)}(\mathbf{r}_m|\varepsilon,\gamma) = & -\sum_{k\notin I_m\cup I'_m} \left\{ \log(\gamma+1) + \frac{|r_m(k)|^2}{\sigma_w^2(\gamma+1)} \right\} \\ & - \sum_{k\in I_m} \log(2\gamma+1) - \frac{(\gamma+1)\Phi_m - 2\gamma Re\{|\Psi_m| \mathrm{e}^{\mathrm{j}(\angle\Psi_m+2\pi\varepsilon)}\}}{\sigma_w^2(2\gamma+1)}, \end{aligned} \tag{18}$$

where $\angle\Psi_m$ denotes the argument of Ψ_m and

$$\Phi_m = \sum_{k\in I_m} [|r_m(k)|^2 + |r_m(k+Q)|^2], \tag{19}$$

$$\Psi_m = \sum_{k\in I_m} r_m(k) r_m^*(k+Q) = |\Psi_m| \mathrm{e}^{\mathrm{j}\angle\Psi_m}. \tag{20}$$

Similarly, the log-likelihood function of (16) can be simplified as

$$\begin{aligned} \Lambda_{\log}^{(2)}(\mathbf{r}_m|\varepsilon,\gamma,\gamma_{1,m}) = & -\log(\gamma^2+2\gamma+1-\gamma_{1,m}^2) \\ & - \frac{(\gamma+1)(|r_{m-L}|^2+|r_{m-L+N}|^2) - 2\gamma_{1,m} Re\{\mathrm{e}^{\mathrm{j}2\pi\varepsilon} r_{m-L} r_{m-L+N}^*\}}{\sigma_w^2(\gamma^2+2\gamma+1-\gamma_{1,m}^2)}. \end{aligned} \tag{21}$$

2.3. Derivation of frequency offset estimator

As shown in (15) and (16), we have one ML cost function for each subset. The total number of ML cost functions from all subsets will be $(2L-1)$. Each ML function can be used to obtain the frequency offset estimate. However, since each subset might contain a different number of OFDM samples, the accuracy of the frequency offset estimate obtained from each ML function might be different. An effective method is then needed to combine the ML functions from all subsets together to derive the frequency offset estimate $\hat{\varepsilon}$.

In order to make a full use of the subsets, we propose an estimator given by

$$\hat{\varepsilon}_I = \arg\max_{\varepsilon}\left\{\sum_{m=1}^{L} \Lambda_{\log}^{(1)}(\mathbf{r}_m|\hat{\gamma},\varepsilon) + \sum_{m=L+1}^{2L-1} \Lambda_{\log}^{(2)}(\mathbf{r}_m|\hat{\gamma},\hat{\gamma}_{1,m},\varepsilon)\right\}, \tag{22}$$

where $\hat{\gamma}$ and $\hat{\gamma}_{1,m}$ are the estimates of γ and $\gamma_{1,m}$, respectively.

From (22), it can be seen that, to obtain the frequency offset estimate, it is sufficient to estimate γ and $\gamma_{1,m}(m=l+1,\ldots,2L-1)$ instead of $\mathbf{h}$, because the proposed estimator can be expressed as a function of γ and $\gamma_{1,m}$ which are related to $\mathbf{h}$, as are given in (14) and (17). In the following, we will show how to obtain $\hat{\gamma}$ and $\hat{\gamma}_{1,m}$.

(1) *The derivation of* $\hat{\gamma}$

In order to obtain $\hat{\gamma}$, a coarse estimator is proposed as follows:

$$\{\hat{\gamma},\hat{\varepsilon}_c\} = \arg\max_{\gamma,\varepsilon}\left\{\sum_{m=1}^{L} \Lambda_{\log}^{(1)}(\mathbf{r}_m|\gamma,\varepsilon)\right\}, \tag{23}$$

where $\Lambda_{\log}^{(1)}(\mathbf{r}_m|\gamma,\varepsilon)$ is given in (18). Note that in (23), only the subsets $\mathbf{r}_m$ for $(m=1,\ldots,L)$ are used for this coarse estimation. Substituting (18) into (23), we obtain

$$\begin{aligned}\{\hat{\gamma},\hat{\varepsilon}_c\} = \arg\max_{\gamma,\varepsilon}\Bigg\{ &-\sum_{m=1}^{L}\Bigg\{\sum_{k\notin I_m\cup I'_m}\left[\log(\gamma+1)+\frac{|r_m(k)|^2}{\sigma_w^2(\gamma+1)}\right] \\ &-\sum_{k\in I_m}\log(2\gamma+1)\Bigg\} - \frac{\gamma+1}{2\gamma+1}\,\Phi + Re\left[\frac{2\gamma|\Psi|e^{j(\angle\Psi+2\pi\varepsilon)}}{\sigma_w^2(2\gamma+1)}\right]\Bigg\},\end{aligned} \tag{24}$$

where $\Phi=\sum_m^L \Phi_m$ and $\Psi=\sum_m^L \Psi_m$.

From (24), we observe that, conditioned on γ, $\sum_{m=1}^{L}\Lambda_{\log}^{(1)}(\mathbf{r}_m|\varepsilon,\gamma)$ achieves the maximum value when $e^{j\angle(\Psi+2\pi\varepsilon)}=1$. Therefore, the coarse estimate of ε can be obtained as

$$\hat{\varepsilon}_c = -\frac{1}{2\pi}\angle\Psi. \tag{25}$$

This coarse frequency offset estimator is actually the frequency offset estimator given in [3] which uses ISI free CP samples to perform frequency offset estimation.

Using (25), and (24) can be further rewritten as

$$\hat{\gamma} = \arg\max_{\gamma}\left\{-\sum_{m=1}^{L}\left\{\sum_{k\notin I_m\cup I'_m}\left[\log(\gamma+1)+\frac{|r_m(k)|^2}{\sigma_w^2(\gamma+1)}\right]-\sum_{k\in I_m}\log(2\gamma+1)\right\} - \frac{\gamma+1}{2\gamma+1}\,\Phi + Re\left[\frac{2\gamma|\Psi|}{\sigma_w^2(2\gamma+1)}\right]\right\}. \tag{26}$$

The estimate of γ can be obtained by solving $d\{\sum_{m=1}^{L}\Lambda_{\log}^{(1)}(\mathbf{r}_m|\gamma)\}/d\gamma=0$. From (26), this is equivalent to solving the following equation:

$$\kappa_0+\kappa_1\gamma+\kappa_2\gamma^2+\kappa_3\gamma^3=0, \tag{27}$$

where $\kappa_0 = (-A\sigma_w^2 - 2D\sigma_w^2 + B + \Phi + 2|\Psi|)$, $\kappa_1 = (-5A\sigma_w^2 - 8D\sigma_w^2 + 4B + 2\Phi + 4|\Psi|)$, $\kappa_2 = (-8A\sigma_w^2 - 10D\sigma_w^2 + 4B + \Phi + 2|\Psi|)$, $\kappa_3 = -4\sigma_w^2(A + D)$ and $B = \sum_{m=1}^{L}\sum_{k\notin I_m\cup I'_m}|r_m(k)|^2$. $A = \sum_{m=1}^{L}\sum_{k\notin I_m\cup I'_m}$ and $D = \sum_{m=1}^{L}\sum_{k\in I_m}$ are counters that count the number of samples defined by the summations.

From (27), $\hat{\gamma}$ can be obtained as

$$\hat{\gamma} = \chi + \left[\frac{\alpha}{2} + \sqrt{\left(\frac{\alpha}{2}\right)^2 + \left(\frac{\beta}{3}\right)^3}\right]^{1/3} + \left[\frac{\alpha}{2} - \sqrt{\left(\frac{\alpha}{2}\right)^2 + \left(\frac{\beta}{3}\right)^3}\right]^{1/3}, \tag{28}$$

where

$$\chi = \frac{\kappa_2}{12\sigma_w^2}, \quad \alpha = \frac{\kappa_1}{\kappa_3} + \frac{\kappa_2^2}{27\kappa_3^2}, \quad \beta = -\frac{2\kappa_2^3}{27\kappa_3^3} + \frac{\kappa_0}{\kappa_3} - \frac{\kappa_2\kappa_1}{3\kappa_3^2}.$$

(2) *The derivation of* $\hat{\gamma}_{1,m}$

Normally, after obtaining $\hat{\gamma}$, $\hat{\gamma}_{1,m}$ can be obtained from (21) following the same procedure presented in the above section. However, we note that, the ML cost function given in (21) is formulated from only two received OFDM samples so that a high estimation error is expected. Here, we propose to compute $\hat{\gamma}_{1,m}$ based on the knowledge of the power delay profile and $\hat{\gamma}$.

(a) *Exponential power delay profile with decaying factor* δ

In this case, $\hat{\gamma}_{1,m}(m = L+1,\ldots,2L-1)$ is given as

$$\hat{\gamma}_{1,m} = \hat{\gamma}\sum_{s=L+1}^{m}\frac{1 - e^{-1/\delta}}{1 - e^{-L/\delta}}e^{-(s-L-1)/\delta}. \tag{29}$$

(b) *Uniform power delay profile*

$$\hat{\gamma}_{1,m} = \frac{(m-L)\hat{\gamma}}{L}. \tag{30}$$

Note that in (29) and (30), we use L rather than L_p to obtain $\hat{\gamma}_{1,m}$. Our simulation results will show later that the algorithm works well even in the presence of inaccurate knowledge of power delay profile.

(3) *The derivation of* $\hat{\varepsilon}$

After obtaining $\hat{\gamma}$ and $\hat{\gamma}_{1,m}$, substituting (18) and (21) into (22), and replacing γ with $\hat{\gamma}$ and $\gamma_{1,m}$ with $\hat{\gamma}_{1,m}$, respectively, the final frequency offset estimator is given as

$$\begin{aligned}\hat{\varepsilon} = \arg\max_{\gamma}\Bigg\{ & -D\log(\hat{\gamma}+1) - A\sigma_w^4(2\hat{\gamma}+1) \\ & - \frac{B}{\sigma_w^2(\hat{\gamma}+1)} - \frac{(\hat{\gamma}+1)\Phi}{\sigma_w^2(2\hat{\gamma}+1)} \\ & - \sum_{m=L+1}^{2L-1}\log[(\hat{\gamma}+1)^2 - \hat{\gamma}_{1,m}^2] + Re\left[\frac{2\hat{\gamma}\Psi e^{j2\pi\varepsilon}}{\sigma_w^2(2\hat{\gamma}+1)}\right] \\ & - \sum_{m=L+1}^{2L-1}\frac{(\hat{\gamma}+1)(|r_{m-L}|^2 + |r_{m-L+N}|^2)}{\sigma_w^2[(\hat{\gamma}+1)^2 - \hat{\gamma}_{1,m}^2]} \\ & + Re\left[e^{j2\pi\varepsilon}\sum_{m=L+1}^{2L-1}\frac{2\hat{\gamma}_{1,m}r_{m-L}r_{m-L+N}^*}{\sigma_w^2[(\hat{\gamma}+1)^2 - \hat{\gamma}_{1,m}^2]}\right]\Bigg\}. \end{aligned} \tag{31}$$

From (31), the frequency offset estimate $\hat{\varepsilon}$ can be obtained as

$$\hat{\varepsilon} = -\frac{1}{2\pi}\angle\left\{\frac{2\hat{\gamma}\Psi}{\sigma_w^2(2\hat{\gamma}+1)} + \sum_{m=L+1}^{2L-1}\frac{2\hat{\gamma}_{1,m}r_{m-L}r_{m-L+N}^*}{\sigma_w^2[(\hat{\gamma}+1)^2-\hat{\gamma}_{1,m}^2]}\right\} = \frac{1}{2\pi}\angle z. \tag{32}$$

Compared with the estimator in [3], our proposed estimator uses all the CP samples rather than only the ISI free CP samples to perform estimation. The frequency offset estimator given in (32) depends on $\hat{\gamma}_{1,m}$. From (29) and (30), we note that in order to obtain $\hat{\gamma}_{1,m}$, the power delay profile should be known to the receiver. The effect of the power delay profile, particularly the effect of L and δ, on the performance of the proposed frequency offset estimator will be investigated in Section 3.

In this study, we begin with ML estimation and end up with an algorithm that only involves the correlation between the CP samples and their data replicas, as shown in (32). Although we have assumed that $N_g \geqslant L$ in the beginning, this is just to ensure a better accuracy. Unlike some of the reported work, our proposed method still can be applied when $N_g < L$. However, it can be seen from (32) that the first term will vanish and the estimator can only use ISI corrupted CP samples to perform estimation. Since practical OFDM systems will use $N_g > L$ [9] to avoid loss of orthogonality, in the following simulations, we only consider the situation when $N_g \geqslant L$. We will show that our proposed algorithm can still give accurate estimation when $N_g = L$.

3. Simulation results and discussions

In this section, we present the results of simulations that are conducted to investigate the performance of the proposed frequency offset estimator given in (32). The samples of one OFDM symbol are collected at the receiver to perform estimation. An OFDM system similar to IEEE 802.11a is used in the simulations. The system and channel parameters are listed in Table 1. Each path gain is generated randomly and is modeled as a complex Gaussian random variable independent of the gains of the other paths. The SNR is defined as $\mathrm{SNR} = \sigma_s^2/\sigma_w^2$. The simulation results are obtained by averaging over 100,000 runs.

First, we investigate the MSE performance of our proposed frequency offset estimator for various SNR and for various number of CP samples. Simulation results are shown in Figs. 2 and 3. From Fig. 2, we can see that as SNR increases, the MSE of our frequency estimator decreases, implying that our estimator is unbiased. Particularly, we plot the MSE performance for the case of $N_g = L$ in Fig. 2. We can also see that, when $N_g = L$, the proposed estimator shows 1–2 dB degradation when compared to the case of $N_g > L$. From Fig. 3, we can further observe that the MSE of our frequency estimators is improved as N_g increases.

Here we also compare the MSE performance achieved by our frequency offset estimator with that achieved by the estimator studied in [1], and the estimator in [3] with only one OFDM symbol being collected for estimation. The simulation results are shown in Fig. 2 for $N_g = L$ and in Fig. 4 for $N_g > L$. From Fig. 2, we observe that when $N_g = L$, our estimator performs better than the estimators in [1,3]. From Fig. 4, we can see that, when $N_g > L$, our frequency offset estimator always outperforms the estimator in [1] which was designed for the AWGN channels. At lower SNR, our estimator performs better than the estimator in [3], while at high SNR, our estimator performs equally well as the estimator in [3]. The reason might be that our proposed estimator exploits all CP samples, while the estimator in [3] uses only ISI free CP samples for estimation. The more samples we use for estimation, the better estimation performance we can expect. Specifically, when $N_g = L$, the estimator in [3] uses only one ISI free sample to perform estimation and thus results in severe performance degradation. From Fig. 4, we can conclude that, with smaller N_g, the performance improvement achieved by our estimator over the estimator in [3] is more significant.

In our algorithm, since L_p is not estimated, the knowledge of L_p is not available at the receiver. We have used the maximum number of delay paths L in deriving the proposed estimator. This does not affect the assumption of uncorrelated neighboring samples in each subset since $L \geqslant L_p$, but it changes the number of summation terms in (26), (32), the number of OFDM samples contained in each subset and the

Table 1
Simulation parameters

N	64
N_g	16
Modulation	QPSK
Channel fading	Rayleigh
Power delay profile	Exponential with decaying factor $\delta = 5$
No. of delay paths	$L = 12$ (unless explicitly stated)

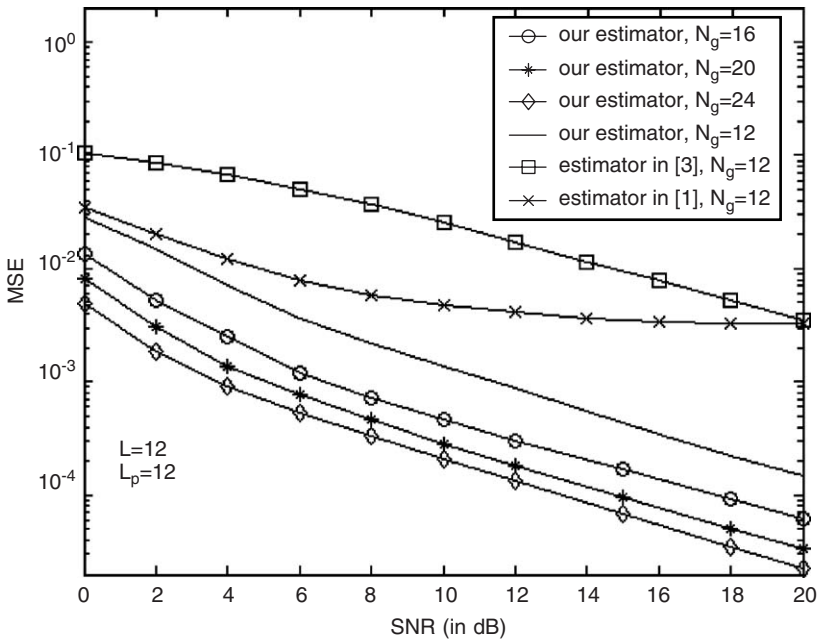

Fig. 2. MSE of proposed frequency estimator versus SNR.

computation of $\hat{\gamma}_{1,m}$. We now investigate how the channel power delay profile affects the MSE performance of our frequency estimator by simulation. Simulation results are shown in Figs. 5 and 6, for $L = 12$ and $N_g = 16$.

From Fig. 5, we can see that when $L_p < L$, the MSE performance degradation caused by unknown L_p is insignificant. The reason causing this insensitiveness of $\hat{\varepsilon}$ to L_p is as follows. On one hand, without the knowledge of L_p, each subset is constructed by picking up the received OFDM samples separated by L rather than L_p samples, the resultant number of OFDM samples in each subset decreases, since $L_p < L$ always holds true. On the other hand, the number of resulting subsets increases with L, since the total number of subsets is given by $2L - 1$. Eventually, almost all the OFDM samples are used in (24) to estimate γ, while almost all the CP samples are used in (32) to estimate ε, like the case of $L = L_p$. To this end, the effect of L_p on the estimate $\hat{\varepsilon}$ will be insignificant.

Next we investigate the effect of decaying factor of δ on the performance of our proposed estimator. In the estimation, the actual $\delta = 5$. Assuming that this knowledge is not known or not correctly estimated by the receiver, instead, $\delta = 3$ and 10 are used to perform estimation. The simulation results are shown in Fig. 6. The results also show that the imperfect knowledge of δ does not cause a noteable performance degradation.

In the following, we attempt to analyze the dependence of the frequency estimate $\hat{\varepsilon}$ on δ by investigating its derivative with respect to δ, or $d\hat{\varepsilon}/d\delta$. Since $\hat{\gamma}$ given in (28) is not an explicit function of δ, based on (32) $d\hat{\varepsilon}/d\delta$

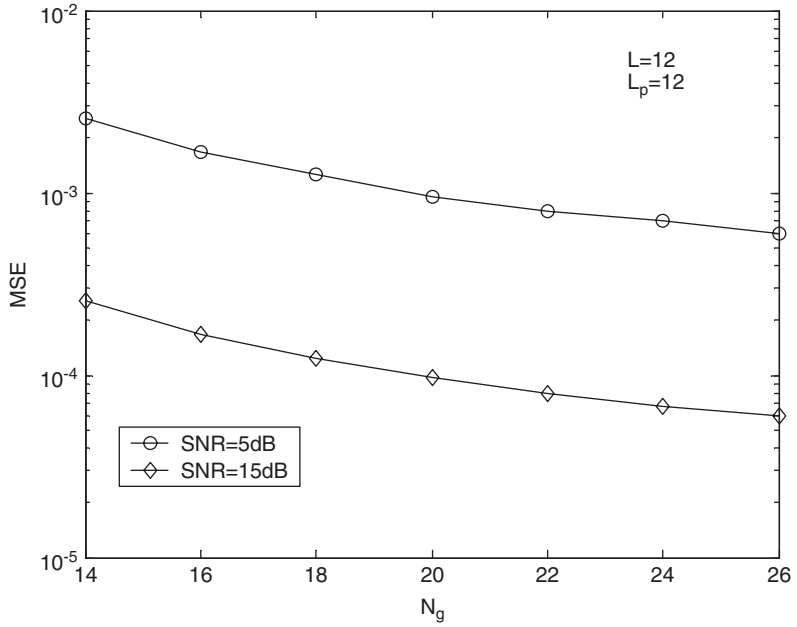

Fig. 3. MSE of proposed frequency estimator versus N_g.

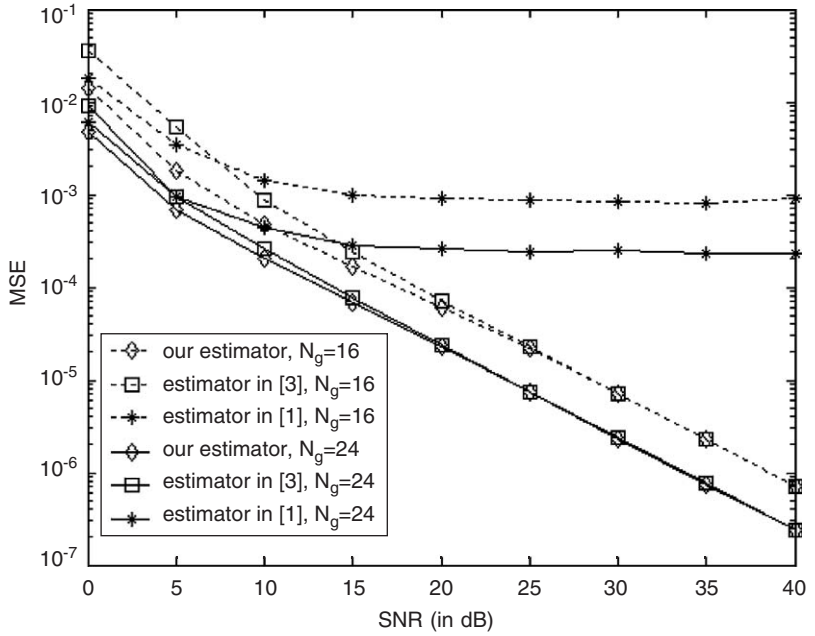

Fig. 4. Comparison of MSE for different estimators.

can be given as

$$\frac{\mathrm{d}\hat{\varepsilon}}{\mathrm{d}\delta} = -\frac{1}{2\pi[Im(z)]^2 + [Re(z)]^2}\left[Re(z)\,\frac{\mathrm{d}[Im(z)]}{\mathrm{d}\delta} - Im(z)\,\frac{\mathrm{d}[Re(z)]}{\mathrm{d}\delta}\right], \tag{33}$$

where $Re(z)$ and $Im(z)$ denote the real and imaginary part of the complex variable z which is given in (32), respectively. Since δ is real, $\mathrm{d}[Re(z)]/\mathrm{d}\delta = Re(\mathrm{d}z/\mathrm{d}\delta)$ and $\mathrm{d}[Im(z)]/\mathrm{d}\delta = Im(\mathrm{d}z/\mathrm{d}\delta)$. To obtain $\mathrm{d}\hat{\varepsilon}/\mathrm{d}\delta$, we only

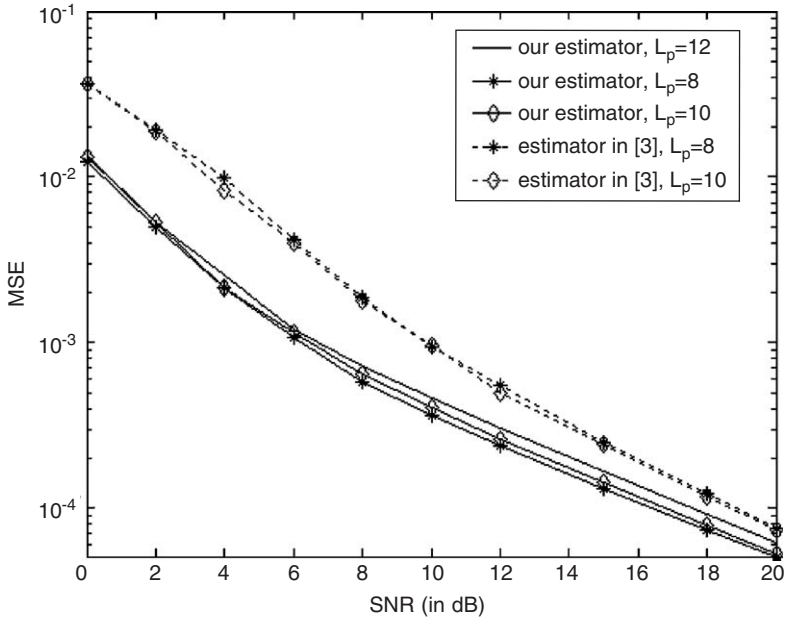

Fig. 5. MSE performance with different L_p.

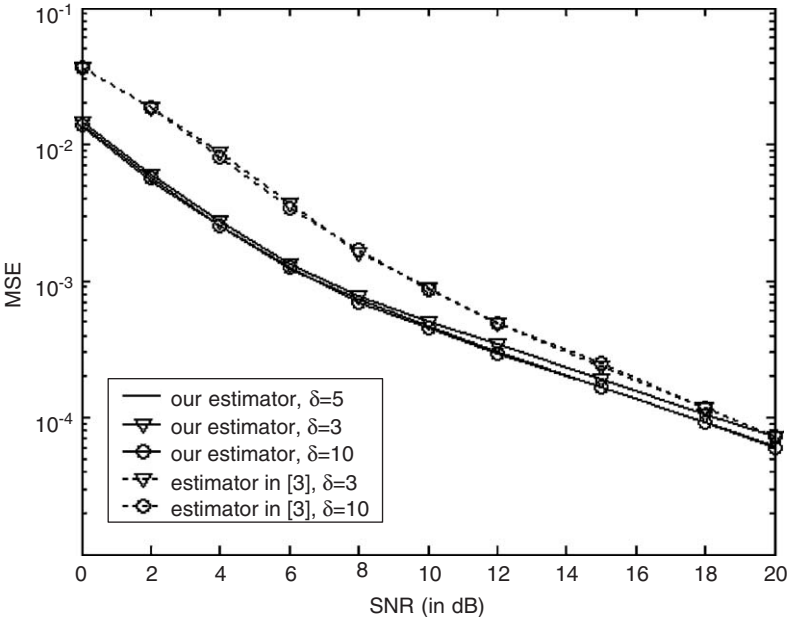

Fig. 6. MSE performance with different δ.

need to derive $\mathrm{d}z/\mathrm{d}\delta$. Using (32), we have

$$\frac{\mathrm{d}z}{\mathrm{d}\delta}=\sum_{m=L+1}^{2L-1}\frac{2r_{m-L}r^{*}_{m-L+N}[(\gamma+1)^2+(\hat{\gamma}_{1,m})^2]}{\sigma_w^2[(\hat{\gamma}+1)^2-(\hat{\gamma}_{1,m})^2]^2}\frac{\mathrm{d}\hat{\gamma}_{1,m}}{\mathrm{d}\delta}. \tag{34}$$

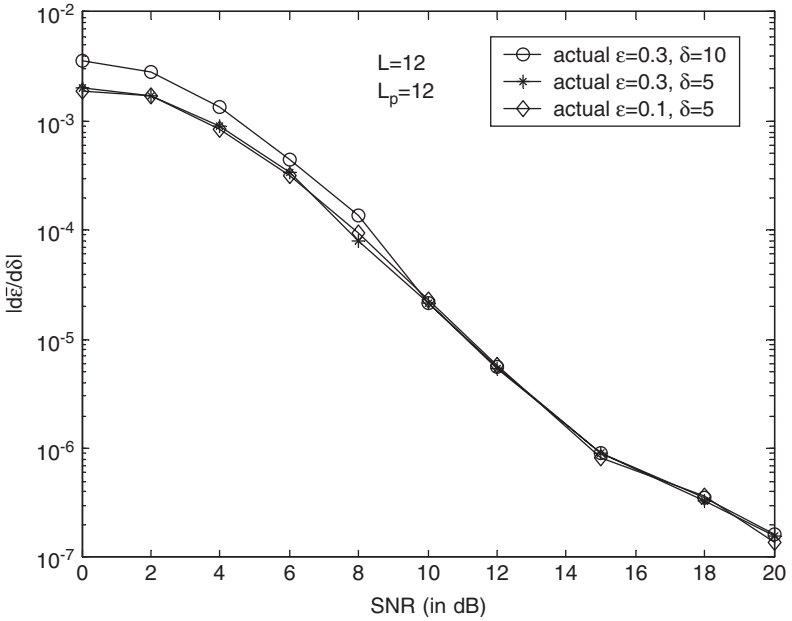

Fig. 7. Effect of $|\mathrm{d}\hat{\varepsilon}/\mathrm{d}\delta|$ for various actual ε and δ.

Based on (29), we have

$$\frac{\mathrm{d}\hat{\gamma}_{1,m}}{\mathrm{d}\delta}=\sum_{m=L+1}^{m}\frac{[1-\mathrm{e}^{-L/\delta}][s-L-1-(s-L)\mathrm{e}^{-1/\delta}]+L[1-\mathrm{e}^{-1/\delta}]\mathrm{e}^{-L/\delta}}{\delta^2\mathrm{e}^{(s-L-1)/\delta}(1-\mathrm{e}^{-L/\delta})^2}. \tag{35}$$

The absolute value of the mean of $\mathrm{d}\hat{\varepsilon}/\mathrm{d}\delta$ or $|E(\mathrm{d}\hat{\varepsilon}/\mathrm{d}\delta)|$ is obtained by simulations and the results are plotted in Fig. 7 for various ε and δ. It can be seen that $|E(\mathrm{d}\hat{\varepsilon}/\mathrm{d}\delta)|$ is of the order of 10^{-3} in low SNR regime (<2 dB in our example), and decreases to the order of 10^{-7} at high SNR regime (>20 dB). For the case of $\varepsilon=0.3, \Delta\delta=5$ (corresponding to the case that the actual $\delta=5$ but $\delta=10$ is used in the estimation), $\mathrm{d}\hat{\varepsilon}\approx 0.01$ for SNR $=0$ dB, $\mathrm{d}\hat{\varepsilon}\approx 10^{-6}$ for SNR $=20$ dB. Compared to the actual frequency offset ε, $\mathrm{d}\hat{\varepsilon}$ is very small. This observation explains the fact that $\hat{\varepsilon}$ is not sensitive to δ.

In conclusion, in this paper, we have proposed a new frequency offset estimator based on the ML principle for OFDM systems over frequency selective fading channels. The proposed frequency offset estimator outperforms the estimator in [1]. At low SNR, the proposed estimator has better MSE performance than the estimator in [3], while at high SNR, our proposed estimator performs equally well as the estimator in [3]. Although the knowledge of channel power delay profile is needed in the derivations of our proposed estimator, simulation results show that the performance of our proposed estimator is not sensitive to the accuracy in estimating the channel power delay profile.

References

[1] J.-J. Van De Beek, M. Sandell, P.O. Borjesson, ML estimation of time and frequency offset in OFDM systems, IEEE Trans. Signal Process. 45 (July 1997) 1800–1805.

[2] T. Lv, H. Li, J. Chen, Joint estimation of symbol timing and carrier frequency offset of OFDM signals over fast time-varying multipath channels, IEEE Trans. Signal Process. 53 (December 2005) 4526–4535.

[3] X. Ma, G.B. Giannakis, S. Barbarossa, Non-data-aided frequency-offset and channel estimation in OFDM: and related block transmission, IEEE ICC'01 (June 2001) 1866–1870.

[4] B. Chen, H. Wang, Blind estimation of OFDM carrier frequency offset via oversampling, IEEE Trans. Signal Process. 52 (July 2004) 2047–2057.

[5] U. Tureli, H. Liu, M.D. Zoltowski, OFDM blind carrier offset estimation: ESPRIT, IEEE Trans. Commun. 48 (September 2000) 1459–1461.
[6] B. Chen, Maximum likelihood estimator of OFDM carrier frequency offset, IEEE Trans. Signal Process. Lett. 4 (April 2002) 123–126.
[7] H. Bolcskei, Blind estimation of symbol timing and carrier frequency offset in wireless OFDM systems, IEEE Trans. Commun. 49 (June 2001) 988–999.
[8] E. Chiavaccini, G.M. Vitetta, Maximum-likelihood frequency recovery for OFDM signals transmitted over multipath fading channels, IEEE Trans. Commun. 52 (February 2004) 244–251.
[9] R. van Nee, R. Prasad, OFDM For Multimedia Wireless Communications, Artech House, Boston, MA, 2000.
[10] H.A. Cirpan, M. Tsatsanis, Stochastic maximum likelihood methods for semi-blind channel estimation, IEEE Signal Process. Lett. 5 (January 1998) 21–24.